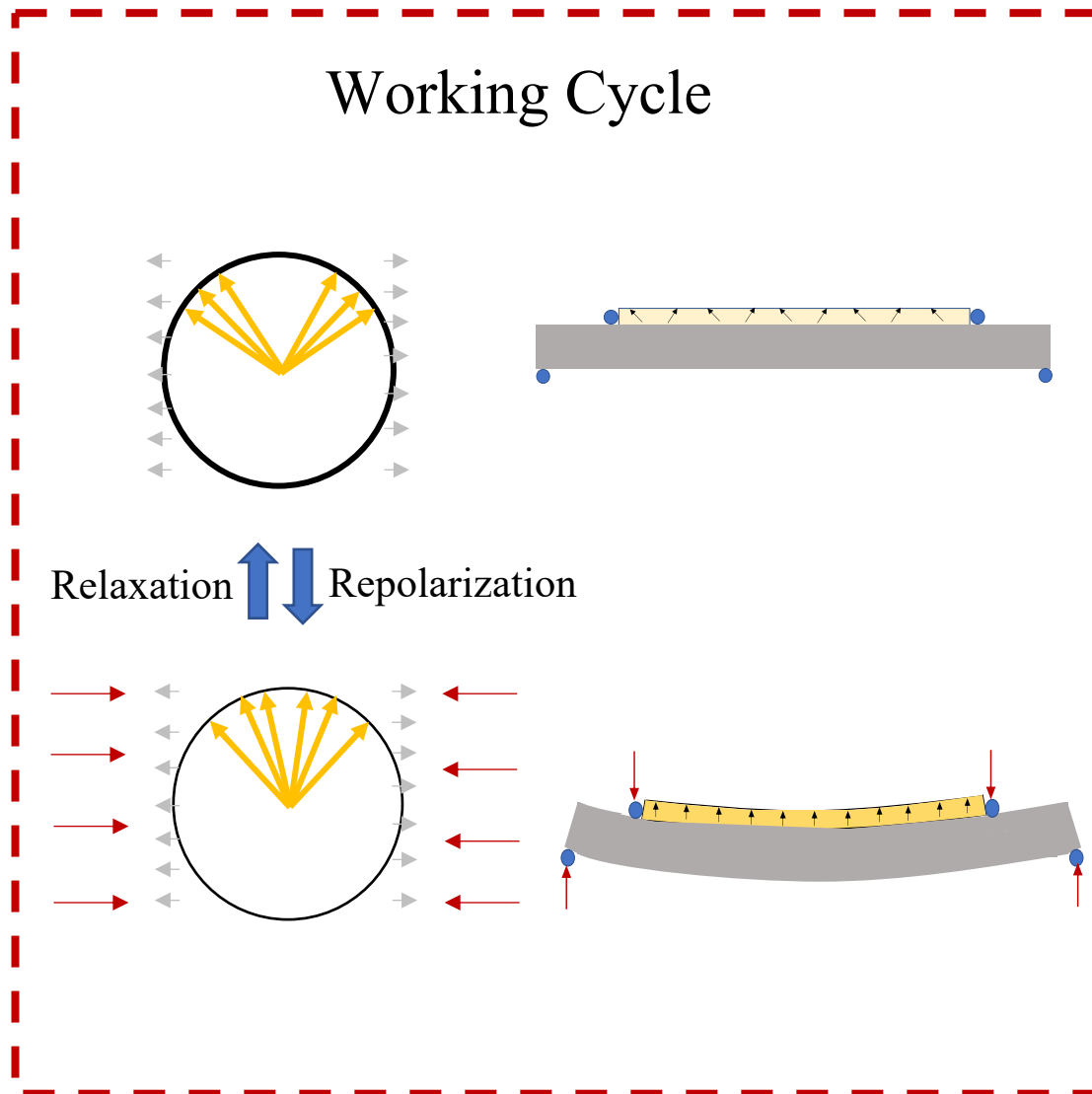


Graphical Abstract

Optimizing a ferroelectric/ferroelastic energy harvester: load impedance and frequency effects

Wenbin Kang ^{*}, Cameron Cain, Robert Paynter, John E. Huber ^{*}



Highlights

Optimizing a ferroelectric/ferroelastic energy harvester: load impedance and frequency effects

Wenbin Kang ^{*}, Cameron Cain, Robert Paynter, John E. Huber ^{*}

- A stable and robust energy harvesting cycle using ferroelectric switching is established.
- The energy harvesting cycle can be optimized by controlling external impedance.
- The optimized average power density can reach 20 mW/cm³.
- The fatigue life exceeds 10⁷ cycles.

Optimizing a ferroelectric/ferroelastic energy harvester: load impedance and frequency effects

Wenbin Kang ^{*a,b}, Cameron Cain^a, Robert Paynter^a, John E. Huber ^{*a}

^a*Department of Engineering Science, University of Oxford, Parks Road, Oxford, OX1 3PJ, United Kingdom*

^b*Physical Intelligence Department, Max Planck Institute for Intelligent Systems, Heisenbergstr. 3, Stuttgart, 70569, Germany*

Abstract

Ferroelectric/ferroelastic switching, which can generate greater charge flows than piezoelectricity for the conversion of mechanical energy into electrical energy, has great potential for novel transducers. However, the requirement for a stable cycle of polarization switching is a challenge for practical applications. Specifically, stress cycles alone do not cyclically vary the remanent polarization of an electroceramic without the assistance of a biasing electric field. In this work, a stress-driven ferroelectric/ferroelastic energy harvester, exploiting internal bias fields in a partially poled ferroelectric, is explored. The harvester is tested and optimized for low-frequency applications, and the effects of electrical load impedance and operating frequency are studied. The device has a simple configuration and offers power density up to about 20 mW/cm³ of active material in the 1-20 Hz frequency range, which is a significant advance over piezoelectric transducers. Additionally, the results show that the energy output at a specific frequency can be optimized through appropriate choice of load impedance, and the optimized cycle works for over 10⁷ cycles at 20 Hz with only slight fatigue degradation. This provides a new perspective for energy harvesting to maximize energy conversion based on ferroelectric/ferroelastic switching with controllable performance.

Keywords: Energy harvesting, Ferroelectric/ferroelastic switching, Design optimization, Electroceramic, Fatigue degradation

Email addresses: kang@is.mpg.de (Wenbin Kang ^{*}), john.huber@eng.ox.ac.uk (John E. Huber ^{*})

1. Introduction

In recent years, the development of electronics has promoted advances in batteries to meet increasing power demands. However, frequent recharging or replacement of batteries is still required to satisfy the demands of portable electronics which now commonly include continuous network access. Hence, energy harvesting technologies, which are eco-friendly and cost-effective, provide an opportunity to replace or support batteries [1, 2, 3, 4]. In the last decade, various kinds of energy harvesting methods, including piezoelectrics [5, 6], pyroelectrics [7, 8] and triboelectrics [9, 10, 11] have been investigated. The energy harvesters scavenge mechanical energy [12, 13, 14], acoustic energy [15, 16], thermal energy [17, 18] or solar energy [19, 20] from the ambient environment. Among these, vibrational energy is clean and sustainable, being available from many sources, including human motion, machines, and fluid flows[21, 22].

The piezoelectric effect has been applied to scavenge mechanical or vibrational energy via electromechanical coupling[23, 24, 25]. Compared with other methods, piezoelectrics provide a simple, solid state generator, without the need for additional components [26]. They can provide high output voltages with very low electrical currents, reducing dissipation. However, the magnitude of loads and displacements is limited in piezoelectric transducers in order to maintain linearity. Consequently, their power density is low. By contrast, triboelectric generators [27] provide a novel transduction mechanism that exploits the separation of electrostatic charge for harvesting mechanical energy, with greater power density than piezoelectrics and diverse, scalable architecture [28, 29, 30, 31]. In 2017, Wang et al. [32] exploited the high dielectric permittivity of a ferroelectric ceramic layer in a triboelectric nanogenerator to enhance its performance. However, the full ferroelectric hysteresis was not used.

Ferroelectric materials possess spontaneous polarization that can be re-oriented through domain wall motion. This can be induced by an external electric field, and is known as ferroelectric switching. Alternatively, stress can induce switching, known as ferroelastic switching [33, 34]. The resulting non-linear changes in shape and polarization can be used to generate electrical work, with greater output than conventional piezoelectric transducers. However, a problem is that, although stress can depolarise an electroceramic, a depolarized electroceramic cannot normally be repolarized by stress. This generally prevents a working cycle in which a cyclic stress could give rise to a

cyclic change of polarization. Some attempts at theoretical energy harvesting designs using combinations of ferroelectric and ferroelastic switching have been developed [35, 36, 37, 38, 39, 40, 41, 42]. Patel et al. [37] proposed a working cycle, wherein a compressive stress depolarizes an antiferroelectric material and repolarization can be carried out by an external electric field. This demonstrated the potential for giant mechanical energy density in electroceramic energy harvesters. Later, Balakrishna and Huber [38] exploited the idea of an engineered domain structure in a nano-layer to design a ferroelectric energy harvester, which uses periodic tensile and compressive stress to drive a charge flow onto and off electrodes. Wang et al. [39, 40] used a phase-field model to improve the design, introducing a bias field to stabilize the working cycles. Kang and Huber [41] subsequently developed an energy harvesting cycle based on bulk polycrystalline ferroelectrics, using tensile stress to depolarize the ferroelectric and electromechanical loading to restore the polarization. This cycle was further analysed and improved by Behlen et al. [42].

Building on these developments, a novel prototype device was proposed by Kang et al. [43, 44] using internal fields instead of externally applied bias fields to direct the polarization changes. The resulting energy harvesters demonstrate high values of energy output and have the advantage of simple structure and operation, similar to established piezoelectric devices. By controlling the polarization state and intrinsic residual tensile stress, only cyclic compressive loading was needed to drive the energy harvester, while partial ferroelectric/ferroelastic switching occurred in each cycle. The fabrication process requires a special step in which partial prepoling of an electroceramic is carried out before it is bonded to a stiff substrate. Afterwards, a strong electric field is applied to complete the poling, and then tensile stress is introduced to partially depolarize the electroceramic. This leaves the ceramic in an electrically and mechanically biased state from which small perturbations can produce significant reversible polarization changes. From this state, compressive loading cycles drive a stable electrical energy output.

The present work extends and develops the energy harvesting method of Kang et al. [43, 44] focusing on the effects of varying electrical load impedance and working frequency. Vibrational tests are reported and a frequency dependent optimum resistive load for maximum energy output is identified. A simplified model based on a piezoelectric energy harvester coupled with an external circuit is presented and used for the interpretation of results. This enables a comparison between the present energy harvester and piezoelectric

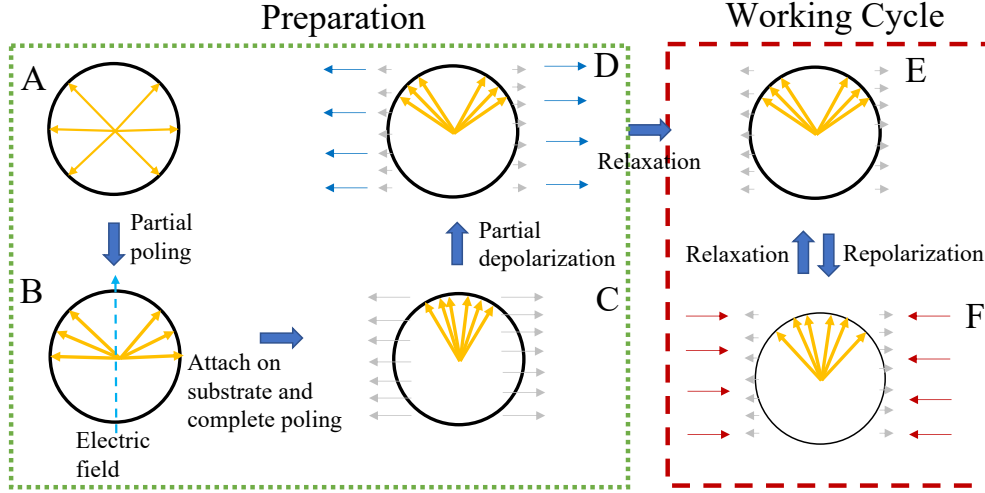


Figure 1: Schematic of cycle and preparation for energy harvesting using ferroelectric/ferroelastic switching. The yellow arrows inside the circles are spontaneous polarizations in the active layer, and the arrays of arrows represent stress. The grey arrow array illustrates residual stress of the active materials, and the blue and red arrows represent tensile loading stress and compressive loading stress respectively. The process from state A to F demonstrates the energy harvesting cycles and preparation. A-B: the active materials are partially polarized; B-C: attach the active materials onto a substrate and complete poling; C-D: partially depolarize the materials by using tensile loading stress; D-E: relax the active layer from the last step; E-F: cyclic compressive loading stress is applied to repolarize the materials and return to the partially depolarized state.

devices. Subsequently, fatigue tests are reported, demonstrating that the optimum energy cycle can be operated without substantial fatigue degradation for more than 10^7 cycles.

2. Design and test arrangement

80 The energy harvester developed by Kang et al.[43, 44] introduces a state of engineered polarization and residual stress to guide the repolarization of a ferroelectric ceramic, resulting in a stable cycle for energy harvesting. The material preparation and working cycle is illustrated in Figure 1. Initially the ferroelectric ceramic is in an unpolarized, as-sintered, state (A in Figure 1). In the first step, the electroceramic is partially polarized to state B using electric field. At this stage there is no mechanical constraint. Then, 85 the partially poled electroceramic is bonded with a stiff substrate, and

the poling is completed by using a strong electric field, producing state C. At C, a transverse residual tensile stress occurs due to blocking of the strain that accompanies polarization changes in the poling process by the substrate. Cracking could occur, but this can be avoided by controlling the degree of prepoling at steps $A \rightarrow B$. Next, tensile stress is applied to the ceramic, reaching state D by causing a partial depolarization. When this load is relaxed (state E) the residual tensile stress is reduced. At state E the material is ready for energy harvesting cycles, wherein the internal fields can provide a preferred direction for repolarization. The energy harvesting cycle starts with the application of a transverse compressive load to partially repolarize the electroceramic to state F. There is a significant change in polarization along the electrical axis during this compression. Relaxation of the compressive load enables material to return to the partially depolarized state. The working cycle moves charge along the electrical axis due to a combination of piezoelectricity and the extrinsic effect of polarization change. An external electrical impedance resists the motion of charge and external electrical work is done. In previous work, cycles with various combinations of mechanical and electrical loading were explored and the degree of prepoling was varied. In the present work, the degree of prepoling was fixed at 30% of the remanent polarization of the fully polarized ceramic, which was found to produce the greatest energy output [43, 44].

For a practical investigation of the energy harvesting cycle, a composite beam arrangement was used, as shown in Figure 2(a). Here, the relaxor ferroelectric, 8/65/35 PLZT, was used as the working material, exhibiting a coercive field of 0.36 MV/m and ferroelastic switching with a coercive stress of approximately 10 MPa[45]. The active material has a 68 GPa Young's modulus and 0.25C/m² remanent polarization at room temperature, with about 1 μ m typical grain size [45]. Relaxor ferroelectrics, with nano-scale domains, combine favourable dielectric and piezoelectric coefficients with low coercive field [46]. The active layer thickness was fixed at 0.33mm and its electroded surface was 38mm \times 4mm. This layer was bonded to a steel substrate of thickness 1mm by a conductive epoxy resin bonding layer less than 0.1mm thick.

Figure 2(b) shows the four-point bending arrangement used for energy harvesting tests. This loading has the advantage of producing a uniform bending moment. Each loading pin is subjected to force $F/2$ which gives rise to approximately uniform uniaxial compression of the ferroelectric layer. A photograph of the fixture mounted in a hydraulic test machine is shown in

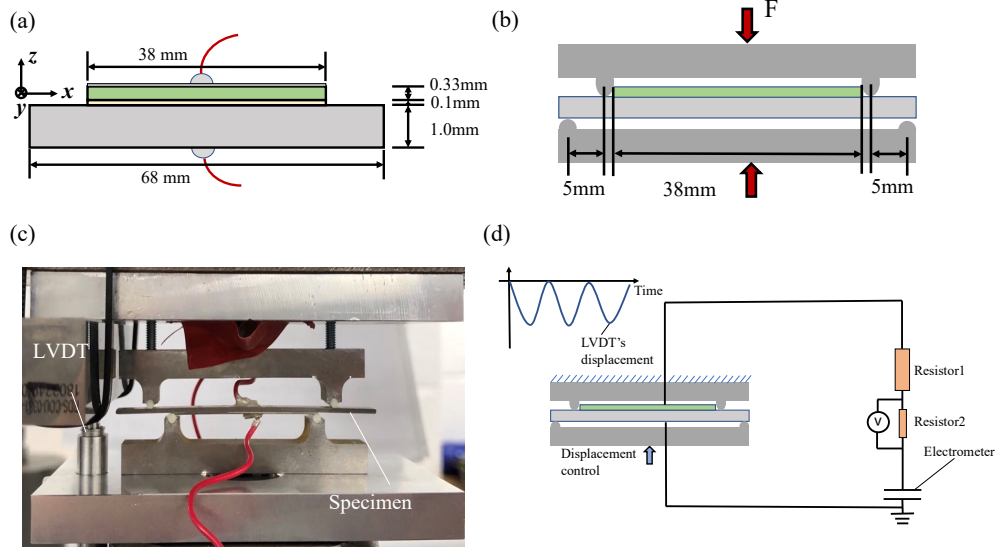


Figure 2: (a) Arrangement of energy harvester (not to scale). (b) Four-point bending arrangement. (c) Four-point bending arrangement using a hydraulic test machine for vibrational tests. (d) Circuit arrangement for vibrational tests.

Figure 2(c). This set-up uses displacement feedback from a linear variable differential transformer (LVDT) to monitor and control the movement of the loading pins. Figure 2(d) shows the external circuit for vibrational tests with resistive loads, and a capacitive electrometer. A potential divider was used such that low voltage measurements across a series resistor indicate current flow from the upper electrode. Vibrational tests were carried out at 1–20Hz, with a range of resistive loads from 3k Ω –15M Ω . Cyclic loading tests, up to 0.55×10^6 cycles at 10Hz and 1.4×10^7 cycles at 20Hz, were run to check for fatigue and the stability of the working cycle.

3. Piezoelectric energy harvester analogue

Modeling of the full ferroelectric and ferroelastic response with non-linear cycles in a partially poled state is challenging. However, a relatively simple piezoelectric model can provide insight into the operating performance of the energy harvester, see figure 3. The model adopts the same structure and loading pattern as the ferroelectric energy harvester, with a uniform bending moment applied along the length of the composite beam.

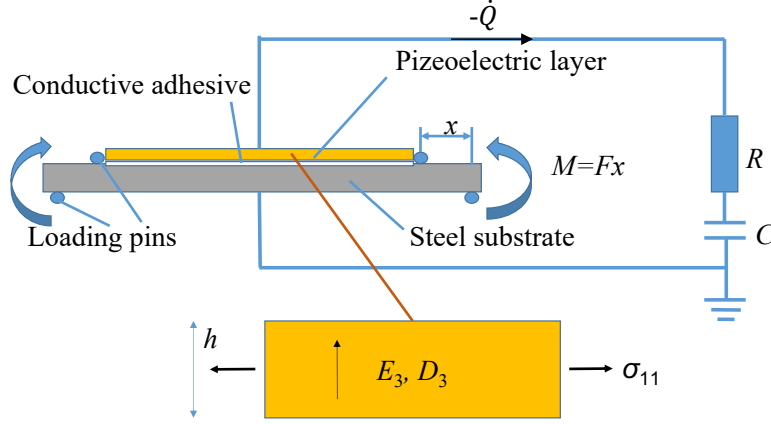


Figure 3: Model of a piezoelectric energy harvester, with structure and loading pattern similar to the ferroelectric energy harvester, coupled with an external circuit.

Euler-Bernoulli beam theory, coupled with the piezoelectric constitutive law is used to model the behaviour of the piezoelectric energy harvester. The piezoelectric governing equation is

$$E_3 = \frac{V}{h} = K_{33}D_3 - g_{31}\bar{\sigma}_{11} \quad (1)$$

where E_3 , V , and h are the electric field in the piezoelectric layer, the voltage at the upper electrode and the thickness of the piezoelectric layer respectively, while K_{33} , D_3 , g_{31} and $\bar{\sigma}_{11}$ represent the dielectric impermeability, electric displacement, piezoelectric coefficient and average stress on the active cross-section, respectively. At any instant, the average stress can be computed directly from the time-varying applied moment $M(t)$ using an integration over the cross section of the composite beam. The electric displacement can be approximated by $D_3 = -Q/A$, in which Q and A are the charge and electrode area respectively. The charge is also proportional to the voltage across the external capacitor. Thus the external circuit provides the relationship

$$-\dot{Q} = \frac{V}{R} - \frac{Q}{CR} \quad (2)$$

where C and R represent the total external capacitance and resistance, respectively. Combining equations 1 and 2 gives the first-order linear differential equation

$$\dot{Q} - \left(\frac{1}{CR} + \frac{hK_{33}}{AR} \right) Q = g_{31}\bar{\sigma}_{11} \quad (3)$$

for the electrode charge Q , in which the average stress $\bar{\sigma}_{11}$ acts as a time varying driving function. In the model, the conductive adhesive layer was treated

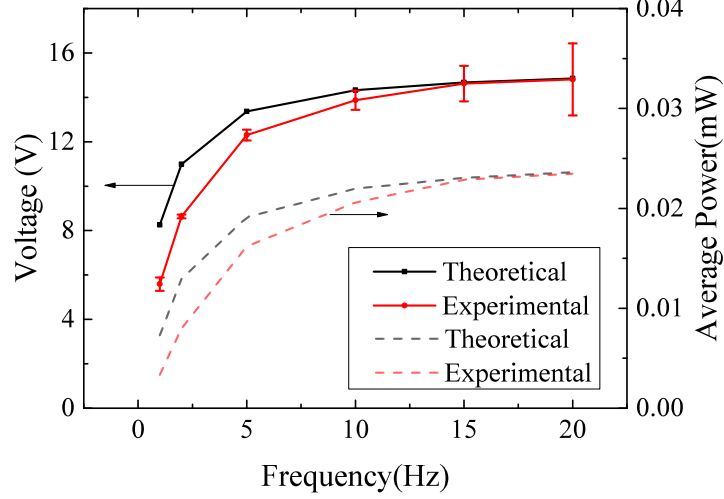


Figure 4: Comparison of the calibrated model results with experimental data using a 100% pre-poled energy harvester.

as a 0.1mm thick elastic layer with Young's modulus 3 GPa and the 1mm steel substrate has Young's modulus 210 GPa. The dielectric impermeability and piezoelectric coefficients, K_{33} and g_{31} , adopt the values of 1.7×10^7 Vm/C and 2×10^{-3} m²/C; a 4.67 M Ω external resistor and a capacitance of 29.62 μ F were used, to match experimental arrangements. The model was calibrated against our experimental set-up using a 100% prepoled energy harvester operating at 20Hz. This device is anticipated to operate largely in the linear piezoelectric regime, but with some non-linearity due to the use of high load amplitude ($F = 30$ N, corresponding to $\bar{\sigma}_{11} \approx 33$ MPa). Model predictions of the voltage and power output, and corresponding experimental measurements are shown in Figure 4. Deviation between the model and experiment at frequencies below 10Hz is attributed to non-linearity in the experiment caused by saturation of the piezoelectric effect at high load levels. In the sequel, this model is used for comparison with the output performance of the ferroelectric/ferroelastic energy harvester.

175 4. Results and discussion

Initial quasi-static tests were carried out to establish a practical range of external impedance values for subsequent testing. Additionally, dynamic tests were used to confirm that the energy harvester was behaving as a non-linear ferroelectric/ferroelastic device - see supplementary material. In
180 practical applications, the impedance of the external circuit will result in a voltage on the ferroelectric layer during energy harvesting. Therefore, the effect of varying the total external resistance was investigated to optimize the performance of the 30% prepoled device. Tests were conducted in the 1–20Hz range, consistent with typical vibrations from human and vehicle
185 motion. The tests were driven using a sinusoidal displacement controlled by LVDT, such that the load varied in the range 0–50N (corresponding to $\bar{\sigma}_{11} = 0\text{--}56\text{MPa}$ compression).

Figure 5 shows the working cycles measured with various resistive loads at 10Hz frequency. The voltage amplitude increases with increasing resistance
190 (figure 5a) but saturates once the resistance is greater than about $5\text{M}\Omega$. The voltage amplitude tends to stabilize as the external resistance approaches an open-circuit condition and current flow becomes negligible. The force versus displacement cycle remains approximately the same in all the tests, as shown in figure 5(b); this is dominated by the substrate stiffness. In figure 5(c),
195 the corresponding electric displacement is presented, showing the collapse of charge flow as the resistance increases.

It is of interest to explore the effect of small resistive loads, as shown in figure 5(d-f), with $50\text{ k}\Omega$, $5\text{ k}\Omega$ and $3\text{ k}\Omega$ total resistance at 10Hz, again driven by a force amplitude of 50N. The resulting voltage amplitudes are similar to
200 those found in quasi-static tests (see supplementary material) but produce stable closed cycles in the dynamic tests at 10Hz, whereas the quasi-static tests produced an open force-electric displacement curve. This suggests that the formation of a stable energy harvesting cycle is dependent on frequency, mechanical amplitude and electrical load.

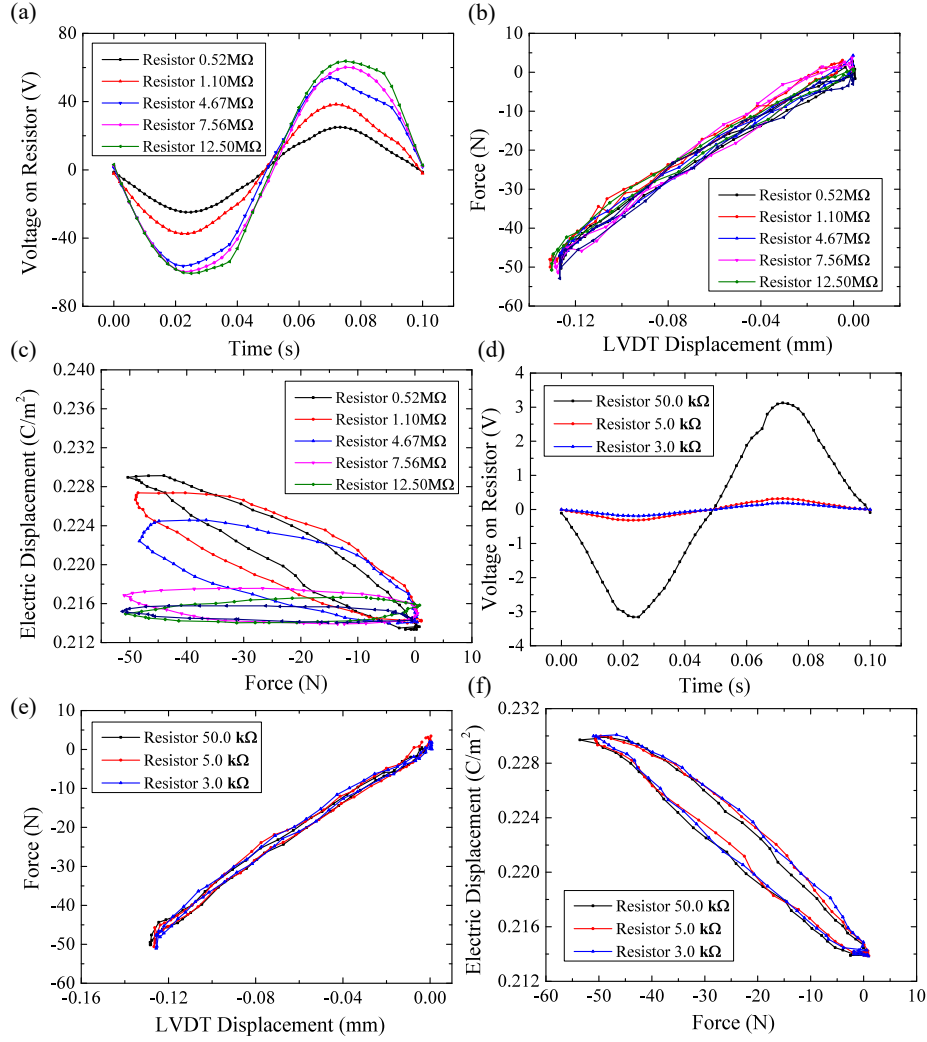


Figure 5: The 30% prepoled energy harvester tested with various resistive loads at 10Hz. (a)(d) Voltage generated across the energy harvester versus time. (b)(e) Force versus LVDT displacement. (c)(f) Electric displacement $-Q/A$ versus force.

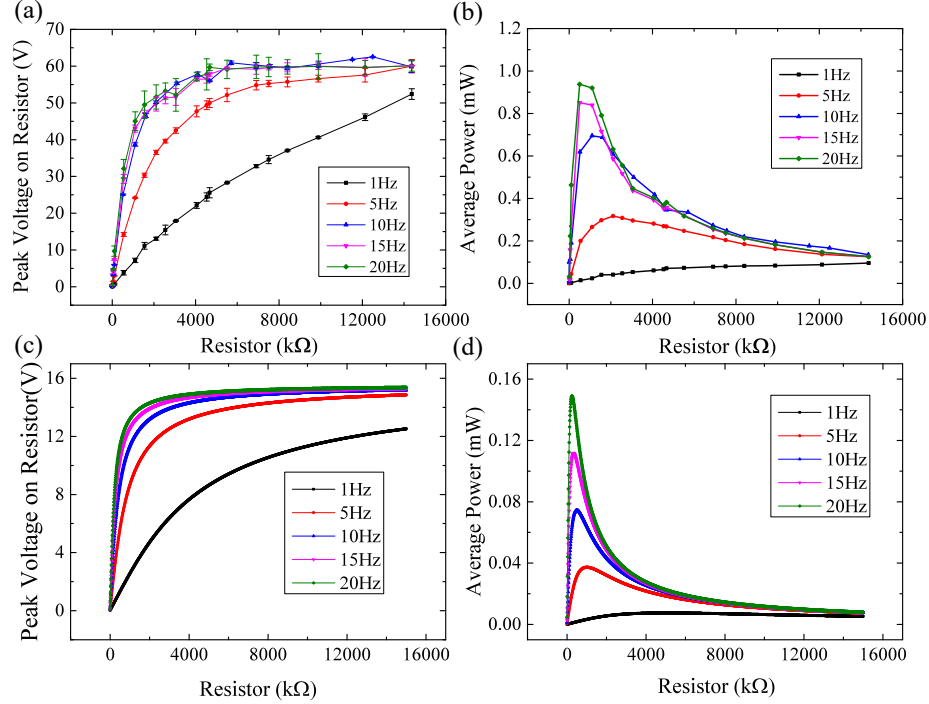


Figure 6: The effect of resistive loads on a 30% prepoled energy harvester at various frequencies(a-b) and model performance of a piezoelectric energy harvester based on the same loading conditions(c-d). (a)(c) Peak voltage. (b)(d) Average power output.

Figure 6(a,b) summarizes results of voltage and power output of the 30% prepoled energy harvester with variation of load resistor and operating frequency. An associated modelling result for the piezoelectric (100% prepoled) energy harvester is shown for comparison in Figure 6(c,d) using the same loading conditions. In the experimental data, the peak voltage increases monotonically with resistance, in a frequency dependent way, rising rapidly at first, followed by a slow rise at greater resistance values. The voltage amplitude stabilizes at about 60V as the open circuit condition is approached, see figure 6(a). In figure 6(b), the average power, obtained by integrating the measured instantaneous power over the cycle, is shown. This indicates that there is a frequency dependent optimum choice of load resistance for maximum power output, as may be expected due to variation of the CR time constant associated with the external resistance and internal capacitance of the energy harvester. The optimal load resistance is sensitive to device size (which controls internal capacitance) and operating frequency. However, it is

220 relatively insensitive to the prepoling condition and mechanical load amplitude, as indicated by figure 6(c,d) where a similar pattern of performance is obtained for a linear model of the 100% prepoled energy harvester. Of interest, the ferroelectric/ferroelastic energy harvester is seen to behave in a way similar to a piezoelectric energy harvester, but with giant voltage and power
 225 output. Effectively, the ferroelectric/ferroelastic device offers characteristics like those of piezoelectrics at low frequency, but with about one order of magnitude greater power density. The average power densities obtained in this work are approximately 14 mW/cm³ at 10Hz and 20mW/cm³ at 20Hz. This suggests that the ferroelectric/ferroelastic device may provide an excellent substitute for traditional piezoelectric transducers in low frequency
 230 applications.

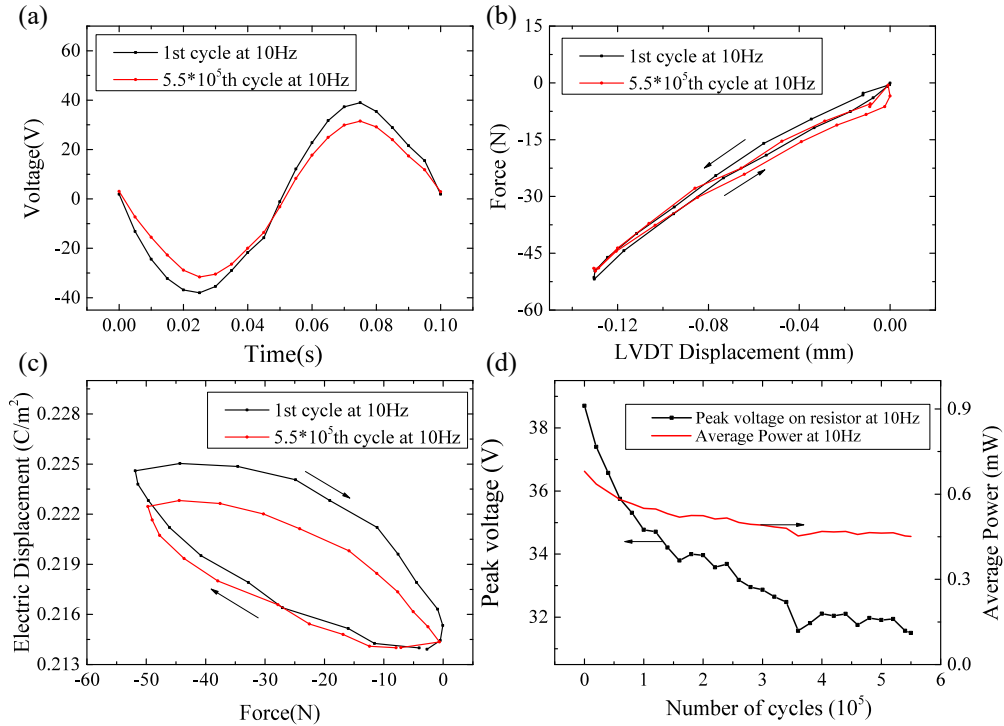


Figure 7: Fatigue testing of the 30% pre-poled energy harvester at 10Hz with a 1.1 MΩ load resistor. (a) Comparison of voltage for 1st and 5.5×10^5 th cycle (b) Corresponding comparison of the mechanical load cycles. (c) Corresponding comparison of the electric displacement versus force cycle. (d) The degradation of peak voltage and power output with cycle number.

To test the fatigue performance of an optimal energy harvesting cycle, loaded with 50N amplitude at 10 Hz, a half million cycles were run using a 1.1 M Ω load resistor. Figure 7 reports the results of the fatigue test, showing some degradation in performance after 0.55×10^6 cycles. The voltage and electric displacement cycles change during cycling, but the system continues to operate with some reduction in voltage and power output, see figure 7(d). The first 10^5 cycles induce a 10% drop in peak voltage, and corresponding 20% change in power output. From 10^5 cycles to 5.5×10^5 cycles, the power output and voltage amplitude decrease slowly and appear to become more stable. During the tests, the energy harvester did not appear to undergo mechanical degradation (no cracks were observed; the mechanical stiffness is almost unchanged), and the energy harvesting cycle operated stably throughout.

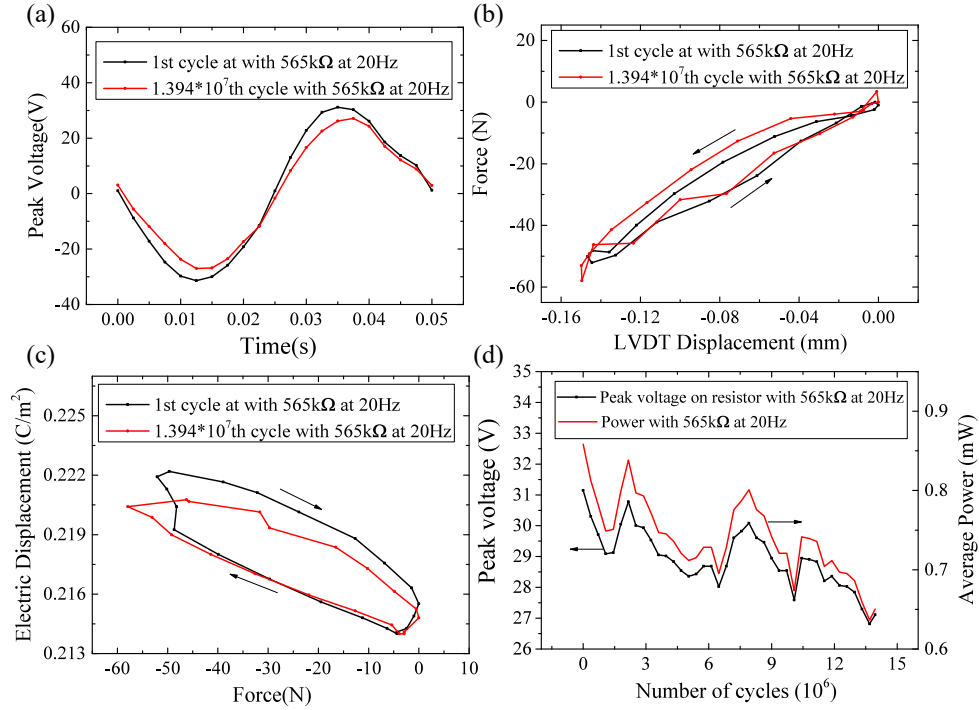


Figure 8: Fatigue testing of the 30% pre-poled energy harvester at 20Hz with a 565 k Ω load resistor. (a) Comparison of voltage for 1st and 1.4×10^7 th cycle (b) Corresponding comparison of the mechanical load cycles. (c) Corresponding comparison of the electric displacement change. (d) The degradation of peak voltage and power output with cycle number.

245 A further fatigue test was carried out at 50 N load amplitude and 20 Hz
 frequency up to 1.4×10^7 cycles. Figure 8 shows the results of this fatigue
 test, again showing a modest degradation in performance. In this test, fluctu-
 ations of the peak voltage and average power were observed, see figure 8(d).
 After 1.4×10^7 cycles the peak voltage had decreased by 13% with an associ-
 250 ated 24% drop in average power. The fluctuations observed may be due to
 slight transverse slip at the loading pins as the position of the energy har-
 vester in the loading fixture was not constrained. Other possibilities include
 variations in ambient temperature or the accumulation of damage. How-
 ever, the key observation is that the device continued to operate with a high
 255 power density for over 10 million cycles, despite operating in a non-linear
 regime with a substantial extrinsic contribution to energy harvesting from
 ferroelectric/ferroelastic switching. This indicates that the device has suffi-
 cient stability and robustness for practical applications. During this test, the
 total energy output of the harvester was approximately 0.5 kJ, equivalent to
 260 about 1.5 times the energy of a typical CR1025 lithium cell.

5. Conclusion

This paper reported the effect of resistive load and operating frequency
 on compressive stress-induced energy harvesting cycles using ferroelectric/
 ferroelastic switching. Following earlier work, the prototype device was fab-
 265 ricated using an off-substrate 30% prepoling process for the active layer,
 followed by complete poling on-substrate. A single cycle of uniaxial ten-
 sile stress was then applied to partially depolarize the ferroelectric. After
 this, working cycles were driven by cyclic compressive stress only. The tests
 in this work demonstrate that there is non-linear switching during the en-
 270 ergy harvesting cycles (extrinsic effect) and provide an understanding of the
 external circuit's influence on ferroelectric/ferroelastic switching. By vary-
 ing the operating frequency in the range 1–20 Hz and changing the electrical
 load, optimized energy output could be identified, with superior performance
 compared to typical piezoelectric transducers operating at low frequency. An
 275 optimized average cycle energy density of 1.4 mJ/cm^3 was achieved at 10 Hz,
 being about an order of magnitude greater than that of typical piezoelectric
 energy harvesters. The results were compared with a model based on piezo-
 electric energy harvesting with the same loading conditions, indicating that
 the ferroelectric/ferroelastic device has a similar load-power characteristic to
 280 a piezoelectric energy harvester but with a much greater effective piezoelec-

tric coefficient. The device operated for over ten million cycles with only modest degradation of performance. This indicates promise for further optimization as a potential alternative to current piezoelectric transducer devices in certain low frequency applications. Finally, it should be noted that optimization of the energy harvester’s structural design, working material and external circuit design for a specific application may yield further performance improvements. The device could readily be adapted to operate with a proof mass for vibration energy harvesting, or to generate pulses of energy from an applied pressure or force. In the present study we have explored its basic performance characteristics to demonstrate the viability of this energy harvesting method.

CRediT authorship contribution statement

Wenbin Kang, John Huber: Provided the design for the experiments and implementation steps. **Wenbin Kang, Robert Paynter:** Experimental set-up establishment. **Wenbin Kang, Robert Paynter, Cameron Cain:** Fabricated the devices, Measured the output performance and analysed data. **Wenbin Kang:** Wrote the manuscript. **John Huber:** Edited the draft. All authors contributed to the manuscript.

Declaration of Competing Interest

The authors declare that they have no known competing financial interests or personal relationships that could have appeared to influence the work reported in this paper.

Acknowledgement

The authors gratefully acknowledge support for Wenbin Kang from the Jardine Foundation.

References

- [1] Y. Liu, H. Zhang, J. Yu, Z. Huang, C. Wang, Y. Sun, Ferroelectric p (vdf-trfe)/poss nanocomposite films: Compatibility, piezoelectricity, energy harvesting performance, and mechanical and atomic oxygen erosion, RSC Advances 10 (2020) 17377–17386.

- [2] L. Yang, D. K. Nandakumar, L. Miao, L. Suresh, D. Zhang, T. Xiong, J. V. Vaghasiya, K. C. Kwon, S. C. Tan, Energy harvesting from atmospheric humidity by a hydrogel-integrated ferroelectric-semiconductor system, *Joule* 4 (2020) 176–188.
- 315 [3] Y. Zhang, X.-J. Song, Z.-X. Zhang, D.-W. Fu, R.-G. Xiong, Piezoelectric energy harvesting based on multiaxial ferroelectrics by precise molecular design, *Matter* 2 (2020) 697–710.
- [4] B. K. Panigrahi, D. Sitikantha, A. Bhuyan, H. Panda, K. Mohanta, Dielectric and ferroelectric properties of pvdf thin film for biomechanical energy harvesting, *Materials Today: Proceedings* 41 (2021) 335–339.
- 320 [5] H. Li, D. Liu, J. Wang, X. Shang, M. R. Hajj, Broadband bimorph piezoelectric energy harvesting by exploiting bending-torsion of l-shaped structure, *Energy Conversion and Management* 206 (2020) 112503.
- [6] N. Sezer, M. Koç, A comprehensive review on the state-of-the-art of piezoelectric energy harvesting, *Nano Energy* 80 (2021) 105567.
- 325 [7] A. Sultana, M. M. Alam, T. R. Middya, D. Mandal, A pyroelectric generator as a self-powered temperature sensor for sustainable thermal energy harvesting from waste heat and human body heat, *Applied Energy* 221 (2018) 299–307.
- [8] H. Ryu, S.-W. Kim, Emerging pyroelectric nanogenerators to convert thermal energy into electrical energy, *Small* 17 (2021) 1903469.
- 330 [9] Z. L. Wang, Triboelectric nanogenerators as new energy technology for self-powered systems and as active mechanical and chemical sensors, *ACS nano* 7 (2013) 9533–9557.
- [10] Z. L. Wang, J. Chen, L. Lin, Progress in triboelectric nanogenerators as a new energy technology and self-powered sensors, *Energy & Environmental Science* 8 (2015) 2250–2282.
- 335 [11] X. Pu, M. Liu, X. Chen, J. Sun, C. Du, Y. Zhang, J. Zhai, W. Hu, Z. L. Wang, Ultrastretchable, transparent triboelectric nanogenerator as electronic skin for biomechanical energy harvesting and tactile sensing, *Science advances* 3 (2017) e1700015.
- 340

- [12] B. Maamer, A. Boughamoura, A. M. F. El-Bab, L. A. Francis, F. Tounsi, A review on design improvements and techniques for mechanical energy harvesting using piezoelectric and electromagnetic schemes, *Energy Conversion and Management* 199 (2019) 111973.
- [13] L. Long, W. Liu, Z. Wang, W. He, G. Li, Q. Tang, H. Guo, X. Pu, Y. Liu, C. Hu, High performance floating self-excited sliding triboelectric nanogenerator for micro mechanical energy harvesting, *Nature communications* 12 (2021) 1–10.
- [14] Y.-H. Shin, J. Choi, S. J. Kim, S. Kim, D. Maurya, T.-H. Sung, S. Priya, C.-Y. Kang, H.-C. Song, Automatic resonance tuning mechanism for ultra-wide bandwidth mechanical energy harvesting, *Nano Energy* 77 (2020) 104986.
- [15] M. Yuan, Z. Cao, J. Luo, X. Chou, Recent developments of acoustic energy harvesting: A review, *Micromachines* 10 (2019) 48.
- [16] G. Ji, J. Huber, Recent progress in acoustic metamaterials and active piezoelectric acoustic metamaterials-a review, *Applied Materials Today* (2021) 101260.
- [17] X. Chen, H. Gao, M. Yang, W. Dong, X. Huang, A. Li, C. Dong, G. Wang, Highly graphitized 3d network carbon for shape-stabilized composite pcms with superior thermal energy harvesting, *Nano energy* 49 (2018) 86–94.
- [18] Y. Zhang, P. T. T. Phuong, E. Roake, H. Khanbareh, Y. Wang, S. Dunn, C. Bowen, Thermal energy harvesting using pyroelectric-electrochemical coupling in ferroelectric materials, *Joule* 4 (2020) 301–309.
- [19] C. X. Guo, G. H. Guai, C. M. Li, Graphene based materials: enhancing solar energy harvesting, *Advanced Energy Materials* 1 (2011) 448–452.
- [20] S.-Y. Chang, P. Cheng, G. Li, Y. Yang, Transparent polymer photovoltaics for solar energy harvesting and beyond, *Joule* 2 (2018) 1039–1054.
- [21] M. A. Abdelkareem, L. Xu, M. K. A. Ali, A. Elagouz, J. Mi, S. Guo, Y. Liu, L. Zuo, Vibration energy harvesting in automotive suspension system: A detailed review, *Applied energy* 229 (2018) 672–699.

- 375 [22] J. Wang, L. Geng, L. Ding, H. Zhu, D. Yurchenko, The state-of-the-art review on energy harvesting from flow-induced vibrations, *Applied Energy* 267 (2020) 114902.
- [23] F. Qian, T.-B. Xu, L. Zuo, Piezoelectric energy harvesting from human walking using a two-stage amplification mechanism, *Energy* 189 (2019) 116140.
- 380 [24] M. R. Sarker, S. Julai, M. F. M. Sabri, S. M. Said, M. M. Islam, M. Tahir, Review of piezoelectric energy harvesting system and application of optimization techniques to enhance the performance of the harvesting system, *Sensors and Actuators A: Physical* 300 (2019) 111634.
- 385 [25] C. Covaci, A. Gontean, Piezoelectric energy harvesting solutions: A review, *Sensors* 20 (2020) 3512.
- [26] S. P. Beeby, M. J. Tudor, N. White, Energy harvesting vibration sources for microsystems applications, *Measurement science and technology* 17 (2006) R175.
- 390 [27] F.-R. Fan, Z.-Q. Tian, Z. L. Wang, Flexible triboelectric generator, *Nano energy* 1 (2012) 328–334.
- [28] L. Fang, Q. Zheng, W. Hou, L. Zheng, H. Li, A self-powered vibration sensor based on the coupling of triboelectric nanogenerator and electromagnetic generator, *Nano Energy* 97 (2022) 107164.
- 395 [29] H.-X. Zou, L.-C. Zhao, Q. Wang, Q.-H. Gao, G. Yan, K.-X. Wei, W.-M. Zhang, A self-regulation strategy for triboelectric nanogenerator and self-powered wind-speed sensor, *Nano Energy* 95 (2022) 106990.
- 400 [30] S. Xu, G. Liu, J. Wang, H. Wen, S. Cao, H. Yao, L. Wan, Z. L. Wang, Interaction between water wave and geometrical structures of floating triboelectric nanogenerators, *Advanced Energy Materials* 12 (2022) 2103408.
- 405 [31] H. Wu, J. Wang, Z. Wu, S. Kang, X. Wei, H. Wang, H. Luo, L. Yang, R. Liao, Z. L. Wang, Multi-parameter optimized triboelectric nanogenerator based self-powered sensor network for broadband aeolian vibration online-monitoring of transmission lines, *Advanced Energy Materials* 12 (2022) 2103654.

- [32] J. Wang, C. Wu, Y. Dai, Z. Zhao, A. Wang, T. Zhang, Z. L. Wang, Achieving ultrahigh triboelectric charge density for efficient energy harvesting, *Nature communications* 8 (2017) 1–8.
- [33] Y. Xu, *Ferroelectric materials and their applications*, Elsevier, 2013.
- 410 [34] L. W. Martin, A. M. Rappe, Thin-film ferroelectric materials and their applications, *Nature Reviews Materials* 2 (2016) 1–14.
- [35] K. Münch, I., C. M. M., Landis, J. E. Huber, Domain engineered ferroelectric energy harvesters on a substrate, *Journal of Applied Physics* 109 (2011) 104106.
- 415 [36] I. Münch, M. Krauß, W. Wagner, M. Kamlah, Ferroelectric nanogenerators coupled to an electric circuit for energy harvesting, *Smart Materials and Structures* 21 (2012) 115026.
- [37] S. Patel, A. Chauhan, R. Vaish, A technique for giant mechanical energy harvesting using ferroelectric/antiferroelectric materials, *Journal of Applied Physics* 115 (2014) 084908.
- 420 [38] A. R. Balakrishna, J. E. Huber, Nanoscale domain patterns and a concept for an energy harvester, *Smart Materials and Structures* 25 (2016) 104001.
- [39] D. Wang, L. Wang, R. Melnik, Vibration energy harvesting based on stress-induced polarization switching: a phase field approach, *Smart Materials and Structures* 26 (2017) 065022.
- 425 [40] D. Wang, R. Melnik, L. Wang, Material influence in newly proposed ferroelectric energy harvesters, *Journal of Intelligent Material Systems and Structures* 29 (2018) 3305–3316.
- [41] W. Kang, J. E. Huber, Prospects for energy harvesting using ferroelectric/ferroelastic switching, *Smart Materials and Structures* 28 (2019) 024002.
- 430 [42] L. Behlen, A. Warkentin, A. Ricoeur, Exploiting ferroelectric and ferroelastic effects in piezoelectric energy harvesting: theoretical studies and parameter optimization, *Smart Materials and Structures* 30 (2021) 035031.
- 435

- [43] W. Kang, L. Chang, J. Huber, Investigation of mechanical energy harvesting cycles using ferroelectric/ferroelastic switching, *Nano Energy* 93 (2022) 106862.
- 440 [44] W. Kang, J. E. Huber, Energy harvesting based on compressive stress-induced ferroelectric/ferroelastic switching in polycrystalline ferroelectric materials, *Cell Reports Physical Science* 3 (2022) 100707.
- [45] C. S. Lynch, The effect of uniaxial stress on the electro-mechanical response of 8/65/35 plzt, *Acta materialia* 44 (1996) 4137–4148.
- 445 [46] A. Bokov, Z.-G. Ye, Recent progress in relaxor ferroelectrics with perovskite structure, *Progress in Advanced Dielectrics* (2020) 105–164.